Lab course Accelerator Bonn (LAB)

Script for the Advanced Laboratory Course (physics601), Experiment E207

Beschleunigeranlage ELSA, Physikalisches Institut, Universität Bonn

version from February 6, 2020

The **L**ab course **A**ccelerator **B**onn setup is a linear, electrostatic electron accelerator specially designed for the advanced laboratory course at the Physics Institute. This experiment is intended as an introduction to the physics and operation of particle accelerators.

The electron beam is emitted by an electron source and accelerated in an electrostatic field to a kinetic energy of 25 keV. Its path and shape along the approximately 3 m long vacuum pipe can be controlled by typical ion optical elements – namely dipole and quadrupole magnets. The resulting beam profiles can be investigated with fluorescence screens.

Procedure and the analysis of the measurements which have to be performed in the lab course are given in section 1. Section 2 gives a brief overview about the setup and short explanations of the individual components. Some basics of accelerator physics and the formalism to describe ion optics are introduced in section 3. The textbook [Wil00] is recommended for a more comprehensive overview. It is available in the library. The script is complemented by a users guide for the control system (appendix A) and a data table with lattice information, which is necessary for the analysis (appendix B).

1. Procedure and Analysis

1.1. Beam Based Alignment

1. **Verify** the **calibration** of the kick angle, which is shown in the control system, of at least two **corrector magnets**: Measure the beam position shift on a screen as a function of the applied corrector kick. If a linear trajectory of the electron beam between the corrector and the screen is ensured, the applied kick angle can be obtained by using the position measurement as well as trigonometric relations. You can use multiple screens to improve your results.

2. **Align the beam** with the corrector magnets so that it is centered horizontally and vertically **in all four quadrupole magnets** applying the beam based alignment method (see section 3.3). Document your measurements and analysis for all quadrupoles in each plane (x and z). E.g. plot the beam position depending on the corrector and quadrupol magnet settings. Record the final kick angles of all corrector magnets.

   ↪ It may be helpful to use the "Toggle Current" feature of the LAB control system, which can be found in the "Magnets" sub menu.

1.2. Emittance Measurement

Characterize the electron beam of LAB using the previously aligned beam line:

1. Determine the horizontal emittance ϵ_x and the vertical emittance ϵ_z via the **quadrupole scan** technique (see section 3.2.1). Measure at least with two quadrupole-screen pairs per plane (x and z).

2. Determine the horizontal emittance ϵ_x and the vertical emittance ϵ_z via the **multi screen** method (see section 3.2.2). Conduct at least one measurement per plane (x and z). Compare your results with those from the Quadrupole Scans.

3. Discuss potential error sources.

Time estimate

- Oral exam/ chat with the tutor: $\approx$ 30min
- Introduction of the experiment by the tutor: $\approx$ 30min
- Beam based alignment: 1h...2h
- Emittance measurement: 2h...3h

2. Overview of LAB

Figure 1 shows a schematic drawing of the total setup, which is divided in four different modules. In this figure the direction of the electron beam goes from left to right.

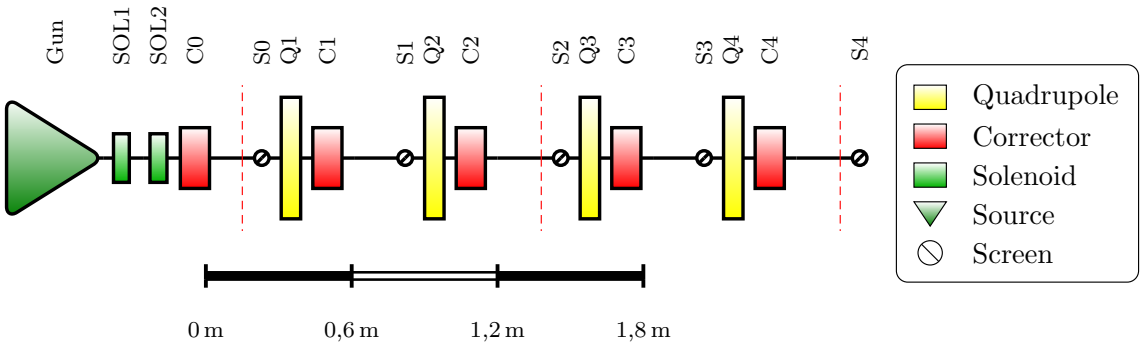

Figure 1: Schematic drawing of the LAB beamline. The red dashed lines indicate the division in four modules.

The first module (left side) consists of an electron source (Gun), two solenoids (SOL1,2) and a corrector magnet (C0). Its purpose is the preparation of an electron beam, initial beam focusing and alignment. The two following modules are identical. Each includes a screen (S), a quadrupole magnet (Q) and a corrector magnet (C). All screens are located in front of a quadrupole magnet to monitor the beam profile and position close to the quadrupoles. At the end of the beamline an additional screen (S4) is mounted.

2.1. Electron Source and Acceleration

The electron source, or electron gun, of LAB was specifically designed and build at ELSA [Höv15]. Figure 2 shows a technical drawing of the electron gun.

Inside an evacuated sphere a cathode and an anode are mounted. The cathode is at high voltage potential while the anode and the whole attached beamline are connected to ground potential. This configuration is called *inverted gun*. The cathode is specially isolated to avoid electric flashovers. The free electrons are generated inside the cathode via thermionic emission from a filament[1]. The initially bound electrons have to overcome the binding energy to leave the material. The required amount of kinetic energy originates from thermal energy, produced by the heating of the filament. The emitted electron rate can be adjusted with the heating current and calculated via the so-called *Richardson equation*.

Figure 3 shows the electrical connections of the electron gun. Since the electrons leave the filament isotropically, an *acceleration* voltage of 10 V to 180 V is applied between filament and cathode. If the filament is set on a negative potential with respect to the cathode, more electrons are accelerated in the direction of the exit hole. A contrary polarity prevents the electrons from leaving the cathode and entering the acceleration field between cathode and anode. So the *acceleration* voltage can be used to switch off the beam. An additional radial electric field is realised by a *Wehnelt* cylinder which is (symmetrically) surrounding the filament, having a negative potential of up to 180 V relative to the cathode exit hole. The radial field configuration of this *focusing* voltage focuses or defocuses the electrons depending on the difference between *focusing* and *accelerating* voltage. Therefore, it can be used to control the beam profile and the number of electrons reaching the exit hole of the cathode.

In general, electron guns are influenced by space charge effects. If a large number of electrons is emitted by the cathode, their charge itself screens the following electrons from the accelerating high

[1] Thin wire, s-shaped bent, material YO_xIr, work function ≈ 2.6 eV.

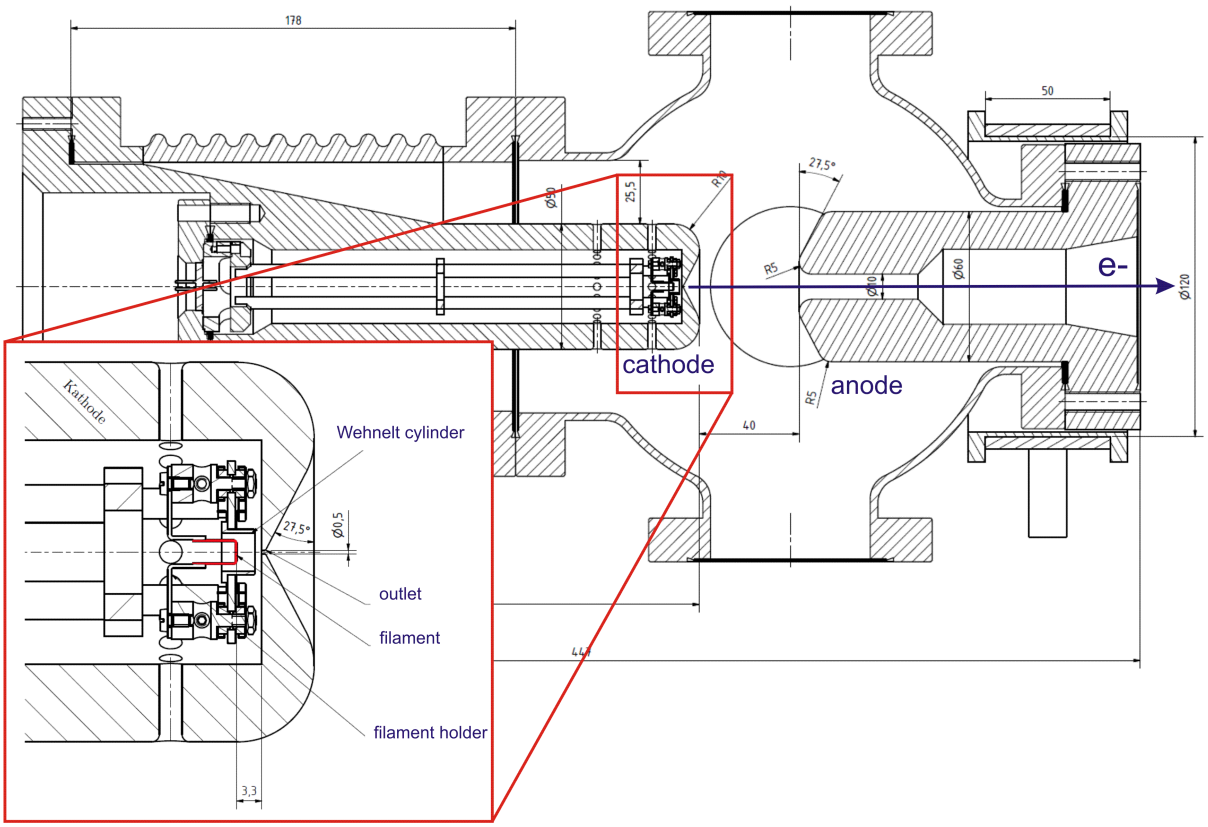

Figure 2: Technical drawing of the electron gun [Hae15]. Linear dimensions are given in millimeters.

voltage. This limits the maximum current of an electron gun depending on the distance of anode and cathode. Furthermore, the charge of the electrons defocuses the beam. This can be compensated by a tapered outer shape of the cathode (*Pearce* angle) introducing a radial focusing component of the accelerating electric field. The electron gun of LAB is operated with an effective emission current of a few µA, leaving the cathode through the 0.5 mm hole. It is not limited by space charge effects.

After leaving the exit hole of the cathode, the electrons are accelerated in a strong electric field caused by the high voltage of typically 25 kV between cathode and anode. The electrons reach $\approx 30.2\,\%$ of the speed of light and enter the 10 mm wide entrance hole of the anode.

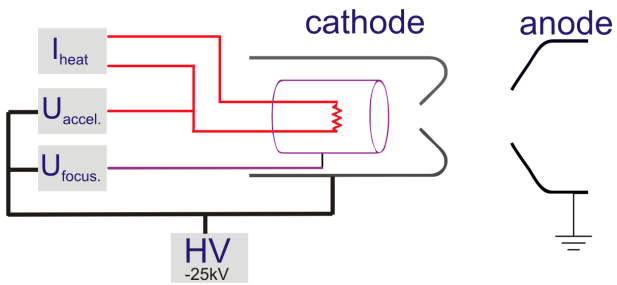

Figure 3: Electrical connections and potentials of the electron gun.

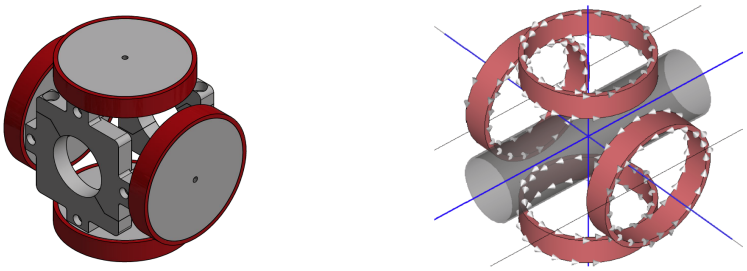

Figure 4: LAB Corrector Magnet. It basically consists of two orthogonally mounted pairs of air-core coils wound around non-ferromagnetic aluminum. Left: [Hae15] Right: [Die15]

2.2. Magnets

Magnets are used to control the beam in particle accelerators. In the same way as photon beams, charged particle beams have to be steered and focused. Hence, particle propagation can be described essentially by a very similar formalism: The concept of ion optics is introduced in section 3.1.

In modern accelerators steering and focusing is realized independently with separate magnet types. Three different types are installed in the LAB beamline and described in the following.

2.2.1. Solenoids

Two solenoids are installed very close behind the electron gun to initially focus the beam. Solenoids are cylindrical coils winded around the beam pipe. They cause a homogeneous magnetic field in longitudinal direction. Electrons with a transverse velocity component are deflected on a helical orbit and additionally focused by the fringe fields (see section 2.2.2). The solenoid acts as thick focusing lens. Further explanation can be found in [Hin08].

2.2.2. Corrector Magnets

The purpose of corrector magnets is to deflect the beam horizontally or vertically. It therefore corrects the horizontal or vertical beam angle and when used in pairs: its position. A small beam deflection can be achieved by an (ideally) homogeneous magnetic field. The correction of the electron beam alignment is necessary to compensate the influence of the earth magnetic field, to overcome possible misalignments of the electron gun and other optical elements, and finally to specifically manipulate the beam direction for any investigations. The bending angle after the passage through the magnetic field can be calculated from the Lorentz force and is given by

$$\alpha \approx \frac{eBL}{p}. \tag{1}$$

Here the small-angle approximation is used, $\vec{B}$ is the magnetic field of the corrector magnet, $\vec{p}$ is the momentum of the electrons and L is the (effective) length of the corrector field. The horizontal and vertical deflection is applied independently as each coil pair induces a vertical or horizontal field. Since the LAB beamline is rather short, they are combined within one mount so that their orthogonal fields superimpose. Figure 4 shows a schematic drawing of the LAB corrector magnet.

The field length L of a magnet is not equal to its physical length (e.g. coils or yoke), because the field strength decreases continuously outside of the magnet – see fig. 5. Therefore the relevant length for all beam dynamics calculations is the effective length L_{eff}, which is the hypothetical length of the constant field B_{max} resulting in the same integrated field along the beam axis (s) as the real field distribution. An effective length of $L_{\text{eff}} = 7.85\,\text{cm}$ was determined for the LAB corrector magnet through a simulation of the field distribution [Die15].

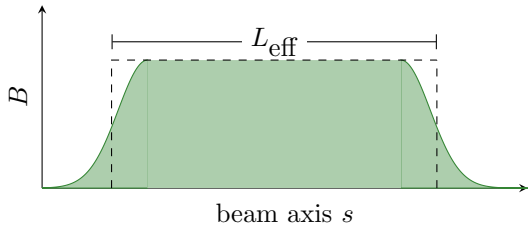

Figure 5: The effective length L_{eff} of a magnet.

The essential technical specification is the maximum integrated field strength achievable with this setup. Here the demand can be estimated from geometrical boundaries to be $(B{\cdot}L)_{\max} \approx 5.14\,\text{mT cm}$. Due to the electron momentum at an acceleration Voltage of max. 50 kV the influence of the earth magnetic field cannot be neglected. The earth magnetic field[2] in Bonn, taking into account an inclination of $\theta_{Bonn} = 66°9'$, is in horizontal direction $B^x_{\text{earth}}(\text{Bonn}) = 19.73\,\mu\text{T}$ and in vertical $B^z_{\text{earth}}(\text{Bonn}) = 44.64\,\mu\text{T}$. This effect has to be fully compensated by the corrector coils, too. Taking this into account, the effective maximum field strength of the corrector coils is in horizontal direction $(B \cdot L)^x_{\max} = 6.3\,\text{mT cm}$ and in vertical direction $(B \cdot L)^z_{\max} = 7.7\,\text{mT cm}$.

Beside a sufficient field strength it is important to realize a homogeneous field along the transverse beam directions. If the field would be inhomogeneous, the strength of the deflection would depend on the transverse position of the electron. The LAB corrector setup is almost a Helmholtz coil configuration[3] (coil radius = coil distance), which provides a $\Delta x = 4\,\text{cm} \times \Delta z = 4\,\text{cm}$ wide region of an almost constant magnetic field strength. This area corresponds to the diameter of the beam pipe. Figure 4 (right) shows the coils' design.

2.2.3. Quadrupoles

While corrector magnets are responsible for beam positioning, beam focusing is achieved with quadrupole magnets. Each quadrupole consists of four magnetic poles with two north poles and two south poles facing each other. Figure 6 shows a cross section of a quadrupole magnet in the transverse plane. The beam axis is perpendicular to it.

The hyperbolic profile of the magnet iron yokes results in a vanishing magnetic field in the center and a field strength increasing linearly with the distance from the center in horizontal and vertical direction. Along the vertical axis (z) the field is oriented horizontally and along the horizontal axis (x) the field points in vertical direction. So the constant field gradients in horizontal (x) and vertical (z) direction are

$$g_x = \frac{\partial B_z}{\partial x}, \qquad g_z = \frac{\partial B_x}{\partial z} \tag{2}$$

and their absolute values are identical for a common symmetric quadrupole. Thus, an electron moving out of the drawing plane with a horizontal displacement in the quadrupole magnet (as shown in fig. 6) experiences a restoring Lorentz force, which is proportional to the displacement. Hence the beam is focused horizontally. Unfortunately the beam is simultaneously defocused by the quadrupole in the vertical plane. If the poles are switched (by changing the sign of the current), the magnet focuses in the vertical, but defocuses in the horizontal plane. It is physically impossible to build a quadrupole magnet which focuses in both planes simultaneously. The solution is so-called *strong focusing*. This concept is well known from optics: A pair consisting of a focusing and a defocusing lens can be used to build an overall focusing system. All modern accelerators use alternating horizontally

[2] Informations about the geomagnetic field can be found here:
`https://www.ngdc.noaa.gov/geomag/WMM/calculators.shtml`

[3] The exact Helmholtz configuration was not possible due to geometrical restritions.

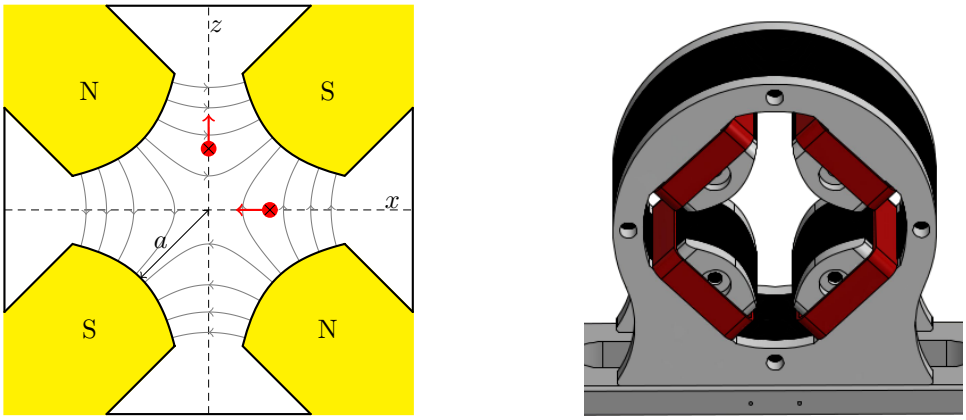

Figure 6: Left: Schematic drawing of a quadrupole setup with hyperbolically shaped pole shoes (yoke). The gray lines indicate the magnetic field lines, while the red arrows show the direction of the Lorentz force, acting upon an electron moving perpendicularly into the drawing plane. The shown magnet is horizontally focusing and vertically defocusing. Right: 3D model of a LAB quadrupole showing the four hyperbolic pole shoes and coils.

and vertically focusing quadrupoles and thereby can focus the beam in both planes. Because of the restoring force along the beamline all electrons perform horizontal and vertical oscillations around the beam center. These can be described mathematically by Hill's differential equations (7) and (8) from section 3.1.2.

The strength of the focusing or defocusing is described by the *quadrupole strength*

$$k = \frac{e}{p} \cdot g = \frac{e}{p} \cdot \frac{\partial B_z}{\partial x} = \frac{e}{p} \cdot 2\mu_0 \frac{n \cdot I}{a^2}, \tag{3}$$

with elementary charge e, electron momentum p, vacuum permeability μ_0, number of coil windings n, current I and half aperture a (see fig. 6). Using the quadrupole strength the magnetic field can be written as

$$B_x = \frac{p}{q} \cdot kz \quad \text{and} \quad B_z = \frac{p}{q} \cdot kx \quad . \tag{4}$$

Similar to the specifications of optical lenses it is possible to define a focal length f depending on the strength k and the length L of the quadrupole:

$$f = \frac{1}{kL}. \tag{5}$$

Using a precisely positioned hall probe the field gradient was experimentally determined to be $g_{\text{meas}} = (0.8501 \pm 0.0009)\,\text{mT/cm}$ [Die15]. Based on section 2.2.3 the quadrupole strength can be calculated considering the current I and the electron momentum p:

$$k = (128027 \pm 150) \cdot \frac{I}{p} \qquad \text{with } [k] = 1/\text{m}^2, [I] = \text{A}, [p] = \text{keV} \quad . \tag{6}$$

An effective longitudinal field length of $L_{\text{eff}} = (7.4 \pm 0.1)\,\text{cm}$ was determined using the hall probe measurements [Die15].

2.3. Beam diagnostics via Fluorescence Screens

The investigations on the transverse beam position and the spot size can be performed with five moveable screens and associated cameras. A screen can automatically be moved into the beam pipe using compressed air. When the electron beam hits the aluminum oxide (Al_2O_3) screen, it emits florescence light in the visible spectral range.

Figure 7 shows a schematic of the setup. The screen is aligned 45 degrees with respect to the beam axis. The fluorescence image of the beam spot is monitored by a CCD camera which is mounted underneath the screen. The analogue video signal is digitized and provided to the control system. Here the intensity distribution of the beam can be determined with a special frame grabber software [Fro15]. Due to the tilt of the screen by 45 degrees, the image magnification factor (conversion pixel to millimeter) is not constant and depends on the vertical position. The resulting distortion of the beam image was experimentally determined [Hof16] and the corresponding calibration is taken into account in the frame grabber analysis software. The screens are located close in front of each quadrupole to monitor the beam position in the quadrupole as accurately as possible.

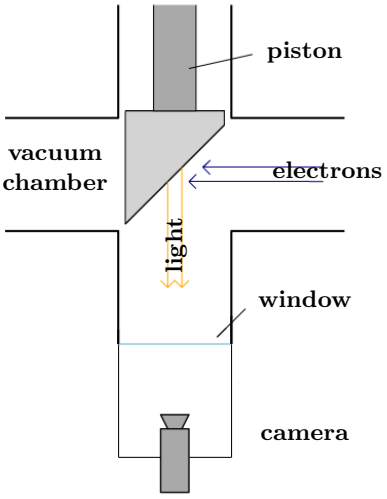

Figure 7: Schematic of a fluorescence screen [Hau15].

2.4. Vacuum system

Since it is important to keep the filament in the electron gun clean and avoid beam quality losses due to collisions with residual gas molecules, the full beam pipe is evacuated. For this purpose an ion getter pump is installed close to the electron gun, which provides a vacuum in the range of 10^{-8} mbar. The vacuum in the following beamline is generated via two additonal turbo molecular pumps, operating in a pressure range of 10^{-7} mbar.

3. Introduction to relevant topics of Accelerator Physics

The following chapter gives an overview of the required background in accelerator physics. The theory includes the description of circular accelerators of which the linar beamline in this laboratory course derives as special case as it misses the *bending* magnets. For this chapter is not as comprehensive as standard textbooks, further literature such as [Wil00] or [Hin08] is recommended.

3.1. Linear Beam Dynamics

3.1.1. Accelerator Coordinates

Particle trajectories in an accelerator are described with a right-handed, curvilinear coordinate system $K = \{x, z, s\}$ (see fig. 8). This means the coordinate system moves along a perfect *design particle* and indicates deviations relative to it, which is useful for circular accelerators. The x- and z-coordinates refer to the horizontal and vertical dimensions whereas s depicts the longitudinal dimension. Note that for negatively charged electrons the *effective* coordinate system becomes left-handed! The magnetic structure within the particles move is referred to as *lattice*.

3.1.2. Hill's Equations

In an accelerator various types of magnets are used to control the particle beam, yet dipole and quadrupole magnets are of fundamental importance and subject of this course. Dipole magnets use a homogeneous field to bend particles to a trajectory with local radius $R(s)$. Wheras the usually larger *bending magnets* in circular accelerators move the coordinate system, its smaller version - the

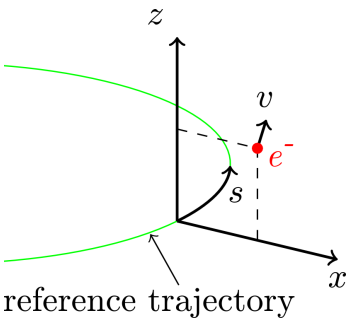

Figure 8: Curvilinear coordinate system describing electron movement within an accelerator structure.

corrector - does not and is used only as correction magnet.
Quadrupole magnets focus the beam with a quadrupole field of strength $k(s)$ (see section 2.2.3).

To sufficiently describe the particle trajectories mathematically within the lattice, linear ion optics can be applied. As simplification, only a constant magnetic field in dipole magnets is taken into account. Furthermore the transverse forces on a particle within quadrupole magnets increases linearly with the particle's deviation from the center of the magnet (cf. section 2.2.3). As an example, the horizontal and vertical equations of motion within a flat circular particle accelerator are given by Hill's differential equations:

$$x''(s) + \left(\frac{1}{R^2(s)} - k(s)\right) \cdot x(s) = \frac{1}{R(s)} \frac{\Delta p}{p} \tag{7}$$

$$z''(s) + k(s) \cdot z(s) = 0. \tag{8}$$

Here x' is defined as $\mathrm{d}x/\mathrm{d}s$, which corresponds to the angle of the particle's motion to the design trajectory (s axis) in the x plane. These differential equations are comparable to those of a mechanical oscillator oscillating around the design trajectory, except that the frequency has a position dependency. In the horizontal case we also find a driving term with dependence on the particle's momentum spread $\Delta p/p$, where Δp is the deviation from the design momentum. As driving of the oscillation occurs only in sections with finite $R(s)$, it is easily identified as dispersion. Note that any magnetic field has dispersive properties, yet the effect from correctors and quadrupoles is neglectable compared to strong bending fields in circular accelerators.

Because LAB is a linear accelerator it has no bending magnets, hence the deflection radius $R(s)$ is infinite for all s and the horizontal differential equation simplifies to the form of eq. (8). Both planes are therefore described in analogy. In the following all equations are written for the horizontal plane (x).

The oscillation of a particle around the design trajectory can be described by the solution of Hill's equations:

$$x_i(s) = A_{x,i}(s) \cos\left(\Psi_x(s) + \phi_i\right), \tag{9}$$

where $A_{x,i}(s)$ is the particle's individual amplitude, $\Psi_x(s)$ its phase advance and ϕ_i the particle's initial phase.

3.1.3. Matrix formalism

To obtain a numerical solution of the particle's trajectory, the matrix formalism is applied. At each position s the vector

$$\vec{x} := \begin{pmatrix} x \\ x' \end{pmatrix}$$

describes a particle's displacement from and angle to the design trajectory in the x plane. Altogether the momentary transverse position and direction of a particle is given by the four dimensional coordinate vector

$$\vec{\mathcal{X}} := \begin{pmatrix} \vec{x} \\ \vec{z} \end{pmatrix} = \begin{pmatrix} x \\ x' \\ z \\ z' \end{pmatrix} \quad .$$

Additionally, the longitudinal motion relative to a design particle can be described by a position shift s and a relative momentum deviation $\Delta p/p$. However, at LAB the electrostatic acceleration and hence the particle momentum stays constant along the whole beamline. As the longitudinal motion is therefore much less complex compared to an accelerator with RF fields for acceleration (see [Wil00]), longitudinal motion is not considered in this script.

Due to the fact that only linear beam dynamics are taken into consideration, it is possible to describe the transverse motion of a particle as a linear transformation of the coordinate vector with a matrix formalism. For a particle with start coordinate $\vec{\mathcal{X}}(s_0)$ it is possible to find a matrix M which includes all optical elements and drift spaces along a path from s_0 to $s_1 = s_0 + \Delta s$ providing the transformation $\vec{\mathcal{X}}(s_0)$ to $\vec{\mathcal{X}}(s_1)$:

$$\vec{X}(s_1) = M \cdot \vec{X}(s_0) \tag{10}$$

$$\begin{pmatrix} x(s_1) \\ x'(s_1) \\ z(s_1) \\ z'(s_1) \end{pmatrix} = M \cdot \begin{pmatrix} x(s_0) \\ x'(s_0) \\ z(s_0) \\ z'(s_0) \end{pmatrix} . \tag{11}$$

The matrix M is called *transfer matrix*. This formalism for linear ion optics is very similar to the well known matrix formalism for geometrical (light) optics. When horizontal and vertical planes are decoupled from each other, the 4×4 matrix M can be decomposed to two 2×2 matrices M_x and M_z describing the horizontal and vertical beam dynamics independently:

$$M := \begin{pmatrix} \boxed{M_x} & \begin{matrix} 0 & 0 \\ 0 & 0 \end{matrix} \\ \begin{matrix} 0 & 0 \\ 0 & 0 \end{matrix} & \boxed{M_z} \end{pmatrix} .$$

In the following the matrices of the optical elements of LAB are described.

Drift Drift sections contain no optical elements, hence particles drift unhindered along this distance. For a drift of length L the transfer matrix reads

$$M_x^{\text{drift}} = M_z^{\text{drift}} = \begin{pmatrix} 1 & L \\ 0 & 1 \end{pmatrix} \quad . \tag{12}$$

Quadrupole magnet Inside a quadrupole magnet the beam is focused in one transverse plane and defocused in the other – as described in section 2.2.3. Typically the quadrupole strengths k is defined so that $k > 0$ refers to focusing in the horizontal plane. Accordingly, a quadrupole is called focusing or defocusing related to its function in the horizontal plane. For a given quadrupole strength $k > 0$ and length L the matrix of a focusing quadrupole magnet is given by

$$M^{\text{QF}} = \begin{pmatrix} \cos\Omega & \frac{1}{\sqrt{k}}\sin\Omega & 0 & 0 \\ -\sqrt{k}\sin\Omega & \cos\Omega & 0 & 0 \\ 0 & 0 & \cosh\Omega & \frac{1}{\sqrt{k}}\sinh\Omega \\ 0 & 0 & \sqrt{k}\sinh\Omega & \cosh\Omega \end{pmatrix} \quad \text{with} \quad \Omega := \sqrt{k}L \quad . \tag{13}$$

For short quadrupoles with small Ω the sin, sinh, cos and cosh terms can be developed in TAYLOR series around $\Omega = 0$ which simplifies the matrices. For example this approximation reduces the term $\sqrt{k}\sin(\Omega)$ to kL, which is equal to the reciprocal focal length $1/f$ (see section 2.2.3). The simplified matrix is then the same as for a thin lens in geometrical optics.

Corrector magnet A horizontal corrector magnet kicks the beam with a kick angle α_x (see section 2.2.2). Here the vector $\vec{x}$ is transformed independently of the particle's displacement and angle via

$$\vec{x}_1 = \vec{x}_0 + \begin{pmatrix} 0 \\ \alpha_x \end{pmatrix} \quad .$$

This cannot be represented by matrix multiplication, therefore the corrector magnet of length L is only represented as a drift without implication on the beam shape describing ion optics.

Transfer matrix of multiple elements With the given matrices for each optical element it is possible to obtain the transfer matrix of an entire beamline from position s_0 to s_1. As in geometrical optics, it is calculated via the matrix product of all element matrices between this distance.

For example, at LAB the transfer matrix from the end of the corrector magnet C0 to the end of corrector C1 is calculated as (compare fig. 1)

$$M_{\mathrm{C0}\to\mathrm{C1}} = M_{\mathrm{C1}} \cdot M_{\mathrm{drift2}} \cdot M_{\mathrm{Q1}} \cdot M_{\mathrm{drift1}}. \tag{14}$$

Note that the matrices are aligned in reverse order to the particle's encounter with these optical elements. The lengths of all elements and drift spaces of LAB can be found in appendix B.

3.1.4. Phase Space, Emittance and Twiss Parameters

For all particles combined, the individual trajectories $x_i(s)$ form *the beam*. Its profile is given by the statistical distribution of the individual particle amplitudes $A_i(s)$ (see eq. (9)). The amplitude of a particle at 1σ of this distribution is used to define the beam envelope $E(s)$ shown in fig. 9.

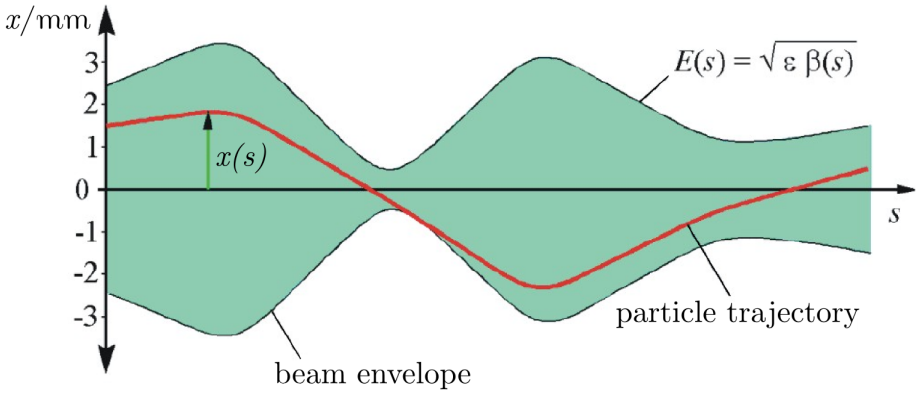

Figure 9: The ensemble of single particle trajectories forms a beam envelope.

It is defined as

$$E(s) = \sqrt{\epsilon \cdot \beta(s)}, \tag{15}$$

where ϵ denotes the so called *emittance*, which is an invariant beam property, and $\beta(s)$ the *amplitude function* or simply *β-function*, which represents the influence of the optical elements on the beam profile. Similar to the *beam parameter product* in Gaussian optics, the invariant ϵ describes the ability to focus the beam. Its statistical meaning becomes more apparent if the beam's displacements x and angles x' are shown *phase space* (x, x') as visualized in fig. 10.

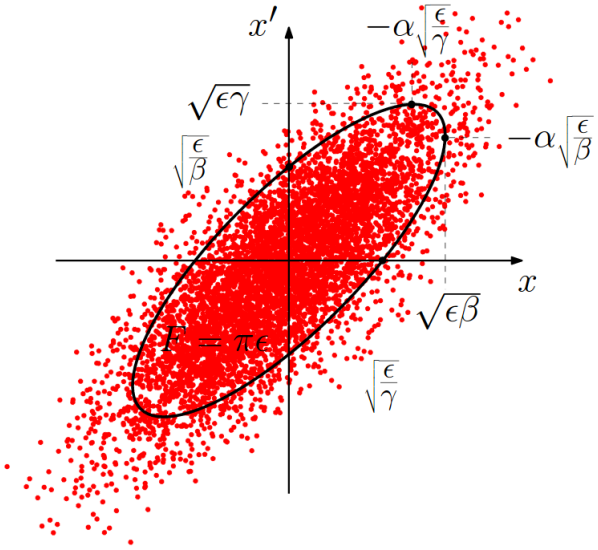

Figure 10: Phase space ellipse in one plane.

When considering the *rms*[4] or 1σ values of the distribution one finds an elliptical shape whose extremal values are described by the *Twiss* parameters α, β and γ. Furthermore the ellipse equation can now be expressed as

$$\epsilon = \gamma(s)\ x_i^2(s) + 2\alpha(s)\ x_i(s) \cdot x_i'(s) + \beta(s)\ x_i'^2(s), \tag{16}$$

where the enclosed area $F = \pi\epsilon$ represents the beam emittance ϵ. According to LIOUVILLE's theorem this area $\pi\epsilon_i$ and thus the emittance is conserved in linear beam optics when only conservative forces are applied. The *Twiss* parameters are related to the phase space distribution of the beam as visualized in fig. 10:

- $\beta(s)$ is connected to the beam width σ_x.
- $\gamma(s)$ is related to the standard deviation of the beam divergence or angular width $\sigma_{x'}$.
- $\alpha(s)$ is a measure for the correlation between $x(s)$ and $x'(s)$.

The three *Twiss* parameters are linked by

$$\alpha(s) = -\frac{\beta'(s)}{2} \qquad \gamma(s) = \frac{1+\alpha^2(s)}{\beta(s)}. \tag{17}$$

The orientation of the phase space ellipse changes across the lattice. Its evolution within a quadrupole magnet and during a drift is illustrated in fig. 11. Note that the ellipse is orientated *upright* or *flat* at the extrema of the beam width, hence at a beam waist or within a quadrupole magnet.

In the case of a Gaussian distribution and a location with an upright ellipse[5], we obtain $\bar{x}_{\text{rms}} = \sigma$, being the Gaussian standard deviation. With $\sigma_x(s)$ and $\sigma_{x'}(s)$ respectively, the beam emittance is now given by

$$F = \pi\ \sigma_x(s) \cdot \sigma_{x'}(s) = \pi\epsilon_x. \tag{18}$$

[4]Root mean square: $\bar{x}_{\text{rms}} = \sqrt{\frac{1}{n}\sum x_i^2}$

[5]beam waist

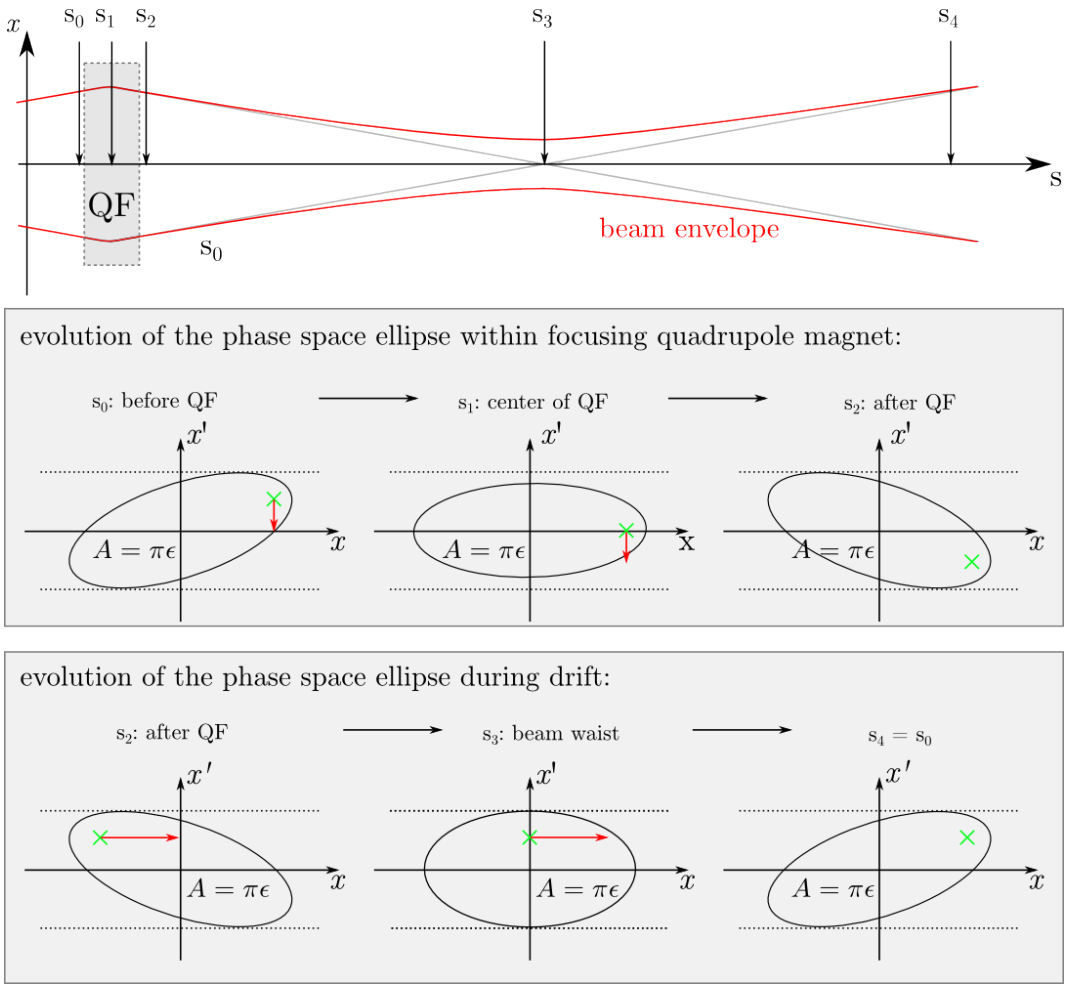

Figure 11: Evolution of the phase space ellipse within a focusing quadrupole magnet and a drift. The orientation changes as the quadrupole alters the angle proportionally to the entrance displacement, whereas the displacement within a drift is continuously altered according to the initial angle. At points of symmetry the ellipse orientation is either *upright* or *flat*.

The local (angular) width of the particle distribution can thus be obtained by

$$\sigma(s) = \sqrt{\beta(s)\epsilon} \qquad \sigma_{x'}(s) = \sqrt{\gamma(s)\epsilon} \qquad r(s) \cdot \sigma(s)\sigma_{x'}(s) = -\alpha(s)\epsilon \tag{19}$$

with $r_x(s) = \frac{\overline{x(s)x'(s)}}{\sqrt{\overline{x^2(s)} \cdot \overline{x'^2(s)}}}$ being the (horizontal) correlation coefficient.

Beta matrix The *twiss parameters* $\beta(s)$, $\gamma(s)$ and $\alpha(s)$ are of great importance for the description and calculation of the beam dynamics in phase space. While the emittance ϵ is a constant property of the beam, the *twiss parameters* depend on the optics of the accelerator and change along the beam axis. They can be transformed using the same transfer matrix M as for the single particle trajectories. For this purpose, they have to be written as the so called *beta matrix* (here for the horizontal plane):

$$B_x(s) := \begin{pmatrix} \beta_x(s) & -\alpha_x(s) \\ -\alpha_x(s) & \gamma_x(s) \end{pmatrix} \quad . \tag{20}$$

Using this, the phase space ellipse equation (see eq. (16)) can be written as the matrix equation

$$\epsilon = (\vec{x}(s))^T \cdot B_x(s)^{-1} \cdot \vec{x}(s) \quad . \tag{21}$$

The *beta matrix* can be transfered with the horizontal 2×2 transfer matrix M_x via

$$B_x(s_1) = M_x \cdot B_x(s_0) \cdot M_x^T \quad . \tag{22}$$

This formalism can be used to calculate the development of the beam width σ_x along a beamline if the accelerator optics (magnet settings) are known. The only free parameter is the emittance ϵ_x which can be measured based on this formalism.

3.2. Emittance Measurements

The emittance ϵ, which was introduced in section 3.1, is an important measure for beam quality since it combines beam width and divergence. It is preserved along the accelerator if the beam energy is not changed. In proton accelerators and linear or low energy electron accelerators it is just determined during beam creation in the gun.

The beam emittance can be determined by measuring the beam width as a function of the beamline settings, especially the quadrupole strengths k. The emittance can then be calculated using the linear beam optics from a starting position s_0 up to the position s_1 where the beam width is measured. This is done with the beta matrix defined in eq. (20). As given in eq. (22) it can be tracked through the beamline by the matrix formalism introduced in section 3.1. The transfer matrix M from s_0 to s_1 yields

$$B_1 = M \cdot B_0 \cdot M^T \qquad \text{with} \quad M := \begin{pmatrix} m_{11} & m_{12} \\ m_{21} & m_{22} \end{pmatrix} \quad . \tag{23}$$

The beam width σ_1 can be expressed by the transformation of the β-function from this equation if it is multiplied with the emittance ϵ:

$$\sigma_1^2 \equiv \epsilon\beta_1 \overset{\text{eq. (23)}}{=} m_{11}^2 \cdot (\epsilon\beta_0) - 2m_{11} \cdot m_{12} \cdot (\epsilon\alpha_0) + m_{12}^2 \cdot (\epsilon\gamma_0) \quad . \tag{24}$$

For a fixed starting position s_0 the beam width σ_1 and the transfer matrix elements m_{ij} only depend on the measurement position s_1 and the strengths k of all quadrupoles between s_0 and s_1. Based on this relation there are two procedures to measure the beam emittance, which are described in the following. Both can be applied for the horizontal emittance ϵ_x as well as for the vertical emittance ϵ_z.

3.2.1. Quadrupole Scan

With the so called quadrupole scan method eq. (24) is measured at a single screen ($s = s_1$) as function of the quadrupole strength k of one quadrupole:

$$\sigma_1^2(k) = m_{11}^2(k) \cdot (\epsilon\beta_0) - 2m_{11}(k) \cdot m_{12}(k) \cdot (\epsilon\alpha_0) + m_{12}^2(k) \cdot (\epsilon\gamma_0) \quad . \tag{25}$$

In thin-lens approxiamtion the value of σ_1^2 changes quadratically as a function of k as the matrix elements then linearly depend on k. The parameters $(\epsilon\beta_0)$, $(\epsilon\alpha_0)$ and $(\epsilon\gamma_0)$ can be determined from a fit. Then the emittance can be calculated using one of the two following approaches:

Emittance via Determinant The first approach makes use of the fact, that the determinant of the beta matrix is one. With the definition of the beta matrix the condition

$$\det(B) = \beta\gamma - \alpha^2 = 1 \qquad \Rightarrow \qquad (\epsilon\beta) \cdot (\epsilon\gamma) - (\epsilon\alpha)^2 = \epsilon^2 \tag{26}$$

can be deduced. Now the fit parameters can be used to calculate the emittance. This ansatz usually is less precise.

Emittance via Measured Beam Waist The second approach uses the transformation of the γ-function

$$\gamma_1 \overset{eq.\ (23)}{=} m_{21}^2 \cdot \beta_0 - 2m_{21} \cdot m_{22} \cdot \alpha_0 + m_{22}^2 \cdot \gamma_0 \quad . \tag{27}$$

In the beam waist, where the beam width is minimal, α is zero and therefore $\gamma_1 = 1/\beta_1$ holds. Insertion in eq. (27) and multiplication with ϵ leads to the expression

$$\epsilon^2 = \sigma_w^2 \left[m_{21}^2(s, k_w) \cdot (\epsilon\beta_0) - 2m_{21}(s, k_w) \cdot m_{22}(s, k_w) \cdot (\epsilon\alpha_0) + m_{22}^2(s, k_w) \cdot (\epsilon\gamma_0) \right] \quad , \tag{28}$$

with the beam width σ_w and corresponding quadrupole strength k_w in the beam waist. They can be determined from the minimum in the measurement.

3.2.2. Multi Screen Method

The so called multi screen method uses eq. (24) with constant quadrupole strengths, but measures the beam width at multiple screens at positions s_i:

$$\sigma^2(s_i) = m_{11}^2(s_i) \cdot (\epsilon\beta_0) - 2m_{11}(s_i) \cdot m_{12}(s_i) \cdot (\epsilon\alpha_0) + m_{12}^2(s_i) \cdot (\epsilon\gamma_0) \quad . \tag{29}$$

This leads to a system of equations with one equation per screen:

$$\underbrace{\begin{pmatrix} \sigma^2(s_0) \\ \sigma^2(s_1) \\ \sigma^2(s_2) \\ \dots \end{pmatrix}}_{\vec{\sigma}} = \underbrace{\begin{pmatrix} m_{11}^2(s_0) & -2m_{11}(s_0) \cdot m_{12}(s_0) & m_{12}^2(s_0) \\ m_{11}^2(s_1) & -2m_{11}(s_1) \cdot m_{12}(s_1) & m_{12}^2(s_1) \\ m_{11}^2(s_2) & -2m_{11}(s_2) \cdot m_{12}(s_2) & m_{12}^2(s_2) \\ \dots & \dots & \dots \end{pmatrix}}_{\mathcal{M}} \cdot \underbrace{\begin{pmatrix} \epsilon\beta_0 \\ \epsilon\alpha_0 \\ \epsilon\gamma_0 \end{pmatrix}}_{\vec{x}} \quad . \tag{30}$$

With more than three screens this system is overdetermined and has to be transformed to a system of three equations via

$$\mathcal{M}^T \cdot \vec{\sigma} = \left(\mathcal{M}^T \cdot \mathcal{M} \right) \cdot \vec{x} \quad . \tag{31}$$

This can be solved for $\vec{x}$. The emittance has to be calculated from the resulting parameters $(\epsilon\beta_0)$, $(\epsilon\alpha_0)$ and $(\epsilon\gamma_0)$ with one of the two approaches described in section 3.2.1. Usually the first approach is applied (eq. (26)), because the beam waist cannot be determined from the measurement. To use the second approach, a beam waist has to be set up at one of the screens before the measurement is conducted.

3.3. Beam Based Alignment

An important procedure for the operation of any accelerator is the alignment of horizontal and vertical beam positions in the center of the beam pipe along the whole beamline. The transverse center of the beam pipe is realistically defined by the center of the quadrupole magnets, where their magnetic field strength is zero. Only if the center of the beam passes a quadrupole centrically, it is focused exclusively. Away from the center the beam experiences an average magnetic field which additionally deflects the beam depending on the field strength (current) of the magnet. Therefore, a beam, which is not centered in a quadrupole magnet, is bent accidentally when changing the quadrupole strength. So proper beam alignment is crucial to decouple beam positioning and focusing.

In real accelerators the beam alignment can never be perfect due to the limited precision of manufacturing and alignment of the gun and all magnets. It is corrected with dedicated correction magnets. The most precise technique for optimizing the alignment is using the beam itself. To center the beam in a quadrupole (in x or z, here x) the following procedure can be used:

1. The kick α_x (current I_x^C) of a corrector magnet in front of the quadrupole is used to set the position where the beam passes the quadrupole.

2. The strength (current) of the quadrupole is varied by a fixed value Δk (ΔI^Q).

3. The resulting beam displacement Δx is measured on a screen behind the quadrupole.

These steps are repeated for different corrector kicks α_x and the displacement $\Delta x(\alpha_x)$ is plotted. The corrector setup for zero displacement can be determined with a linear fit. This procedure can be applied step by step for each quadrupole to obtain a well aligned beamline.

A. Quick Users Guide: ELSA control system

A.1. Device Operation

LAB is controlled through a modified version of ELSA's control system GUI[6] (fig. 12). It is opened via the desktop icon or from the corresponding task bar button.

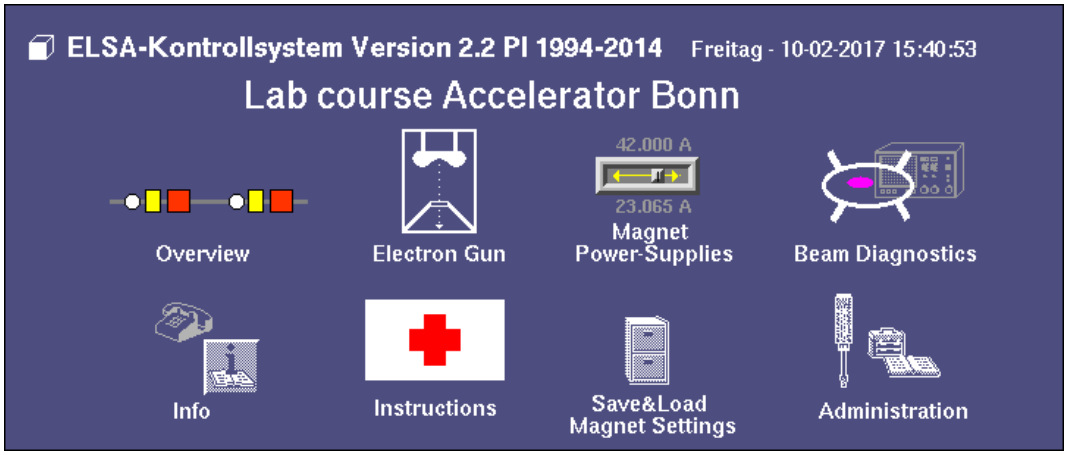

Figure 12: LAB's control system main menu.

As the control system usage is mostly intuitive, a few hints may improve the handling as depicted in fig. 13. Note that it is always recommended to save a value to its individual memory before it is altered. Saving the global status is described below.

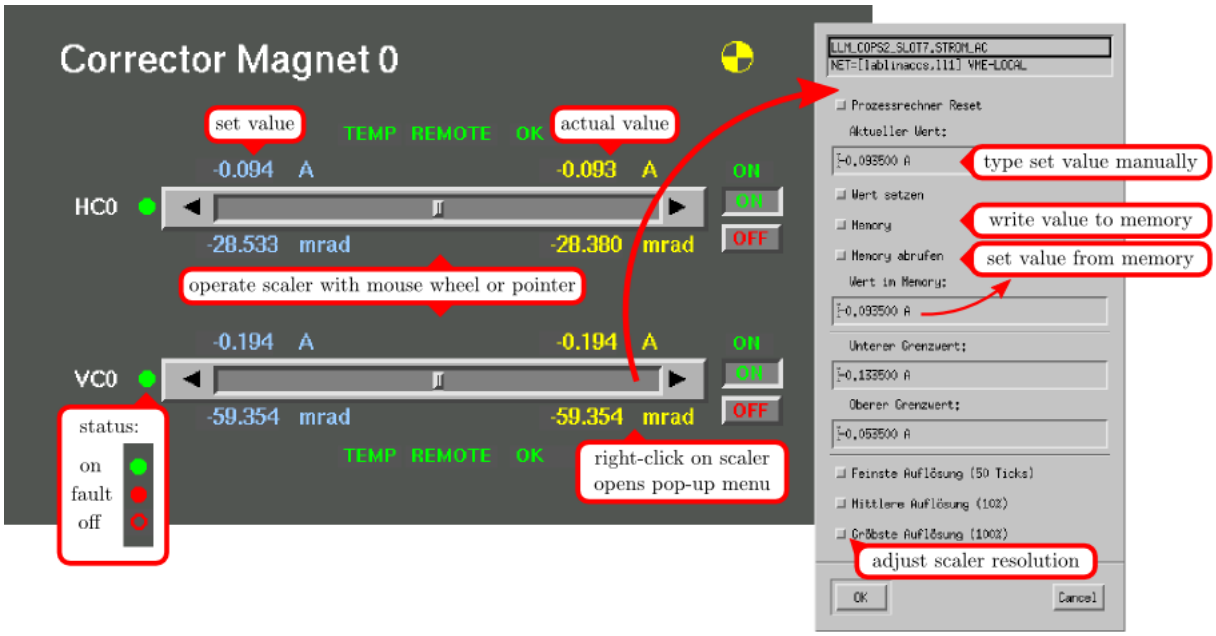

Figure 13: Typical device operation menu with status, value slider, set (blue) and get (yellow) values. A pop-up opens with right-click on slider to enter values manually, save and get them from memory and to adjust slider resolution.

[6] graphical user interface

A.2. Save and Load Machine Settings

During the lab session various beam optics scenarios are examined. To quickly return to useful global machine settings – after e.g. missteering the beam – sets of magnet values can be saved, commented and restored via the main menu through *Save & Load Magnet Settings* (see fig. 14).

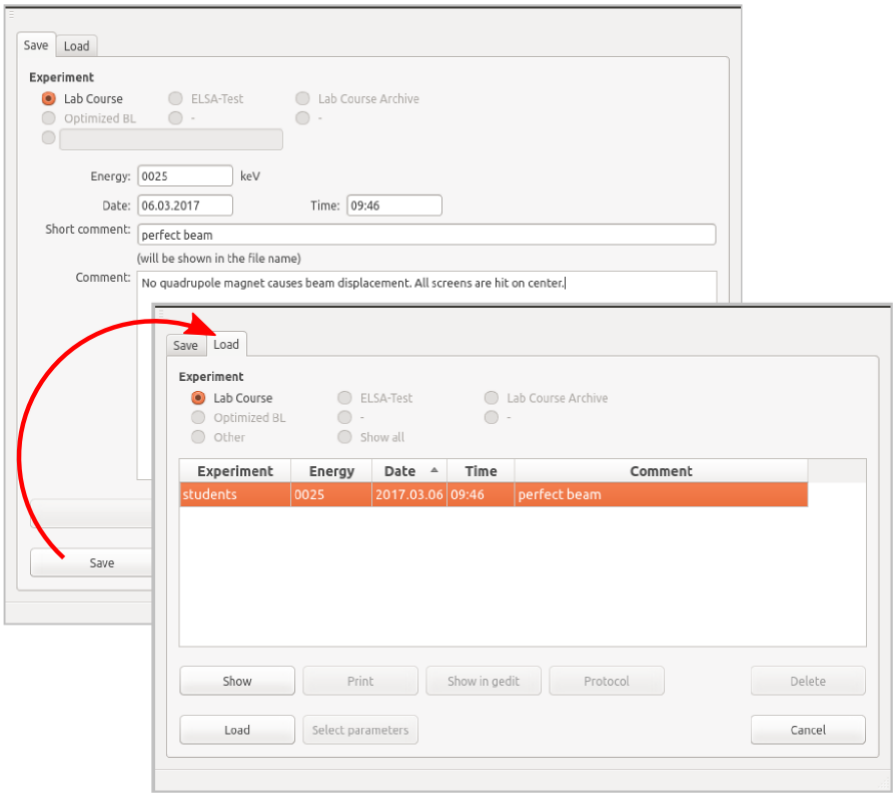

Figure 14: Save and load magnet currents for documentation and to return to operational settings.

A.3. Beam Images and Frame Grabber Settings

The beam profile and intensity measurements from the digitized CCD images are processed by an in-house developed frame grabber analysis software (fig. 15):

① Start the frame grabber from the *main menu* → *Beam Diagnostics* → *Framegrabber*.

② To obtain an image, a flourescence screen must be inserted and the *Start* button in the frame grabber menu pressed.
↪ Contrast & brightness adjustment as well as image averaging (*Add images*) will help to suppress background noise and improve the fit quality.

③ The image is shown in an additional window where an area of interest (AOI) or lines of interest (LOI) can be dragged and resized around the beam image area.
↪ Best values are obtained if AOI and LOIs roughly match the image size.

④ The obtained profile can be checked by opening the relevant AOI *Windows*.
↪ If LOI profiles are saturated (e.g. distinctive flat-top), the fit quality will decrease.

⑤ Different fit functions can be selected via *Control of AOIs*.
↪ *Gauss function* is recommended, yet other functions may be helpful in certain cases.

⑥ The fit values are available in *main menu* → *Beam Diagnostics* → *Beam Profile*, if *Send data to CCS* is selected.
↪ The measurement errors are to this point in an experimental stage. Add useful error estimation to your records.

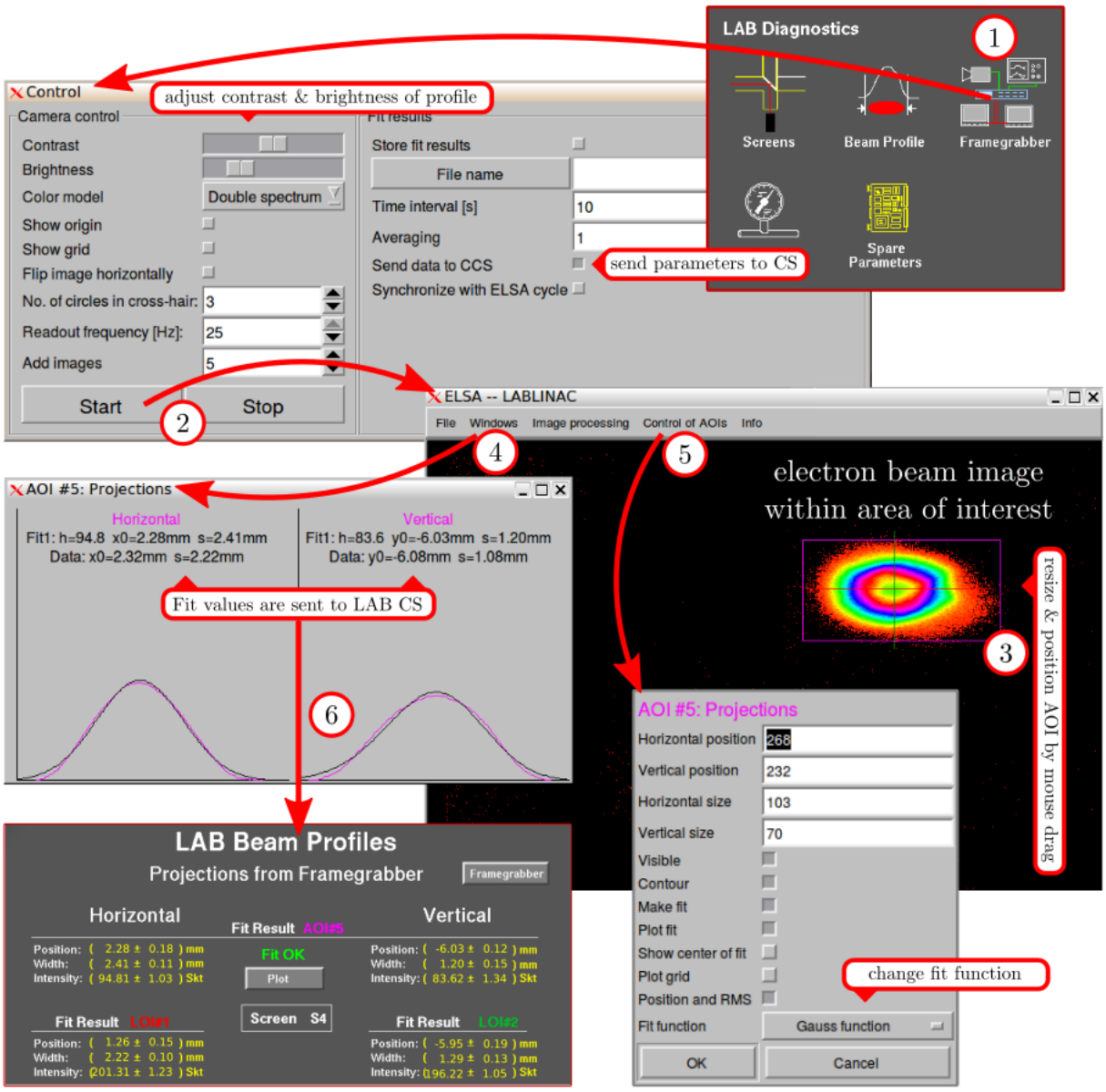

Figure 15: Framegrabber menu, beam image, profiles and adjustment menus.

B. LAB Lattice Data

B.1. Element and Drift Lengths

The following table contains the lengths of all elements in the LAB beamline and the drift spaces between them. In case of the magnets the given lengths are the effective field lengths (see fig. 5). These information should be used for matrix optics calculations.

name	type	length / m
C0	corrector	0.0785
	drift	0.185
S0	screen	0.04
	drift	0.06
Q1	quadrupole	0.074
	drift	0.03
C1	corrector	0.0785
	drift	0.316
S1	screen	0.04
	drift	0.06
Q2	quadrupole	0.074
	drift	0.03
C2	corrector	0.0785
	drift	0.316
S2	screen	0.04
	drift	0.06
Q3	quadrupole	0.074
	drift	0.03
C3	corrector	0.0785
	drift	0.316
S3	screen	0.04
	drift	0.06
Q4	quadrupole	0.074
	drift	0.03
C4	corrector	0.0785
	drift	0.316
S4	screen	0.04

B.2. Magnet Parameters

Corrector Parameters	
coil geometry	round
coil radius	40 mm
number of windings	300 (in 8 layers)
coil distance	105 mm
wire diameter	0.3 mm
physical length L_{phys}	80 mm
effective field length L_{eff}	78.5 mm

Quadrupole Parameters	
coil geometry	rectangular
coil edge length	52 mm × 72 mm
number of windings	120 (in 4 layers)
half aperture a	28 mm
wire diameter	0.3 mm
physical length L_{phys}	(71.3 ± 0.5) mm
effective field length L_{eff}	(74 ± 1) mm

References

[Die15] Yannick Dieter. "Magnetoptik des Laborbeschleunigers LAB". Bachelorarbeit. Universität Bonn, July 2015.

[Fro15] Frank Frommberger. ELSA: Control System - FrameGrabber. Communications. 2015.

[Hae15] Philipp Haenisch. ELSA: Technical drawings. Communications. 2015.

[Hau15] Philip Hauer. "Ansteuerung und Strahldiagnose des Laborbeschleunigers LAB". Bachelorarbeit. Universität Bonn, July 2015.

[Hin08] Frank Hinterberger. Physik der Teilchenbeschleuniger und Ionenoptik. Springer-Verlag, 2008.

[Hof16] Martin Kurt Hoffmann. "Strahldiagnose und Strahloptik am Laborbeschleuniger LAB". Bachelorarbeit. Universität Bonn, Sept. 2016.

[Höv15] Thilo vom Hövel. "Aufbau, Untersuchung und Inbetriebnahme einer Elektronenquelle für den Laborbeschleuniger LAB ". Bachelorarbeit. Universität Bonn, Aug. 2015.

[Wil00] Klaus Wille. The Physics of Particle Accelerators: An Introduction. Clarendon Press, 2000.